



Molecular Crystals and Liquid Crystals Incorporating Nonlinear Optics

Publication details, including instructions for authors and
subscription information:

<http://www.tandfonline.com/loi/gmcl17>

Phase Equilibria in Mixtures Containing Polystyrene and Nematic Liquid Crystals

J. R. Dorgan^a & D. S. Soane^a

^a Department of Chemical Engineering, University of California,
Berkeley, Berkeley, CA, 94720, U.S.A.

Version of record first published: 04 Oct 2006.

To cite this article: J. R. Dorgan & D. S. Soane (1990): Phase Equilibria in Mixtures Containing Polystyrene and Nematic Liquid Crystals, *Molecular Crystals and Liquid Crystals Incorporating Nonlinear Optics*, 188:1, 129-146

To link to this article: <http://dx.doi.org/10.1080/00268949008047811>

PLEASE SCROLL DOWN FOR ARTICLE

Full terms and conditions of use: <http://www.tandfonline.com/page/terms-and-conditions>

This article may be used for research, teaching, and private study purposes. Any substantial or systematic reproduction, redistribution, reselling, loan, sub-licensing, systematic supply, or distribution in any form to anyone is expressly forbidden.

The publisher does not give any warranty express or implied or make any representation that the contents will be complete or accurate or up to date. The accuracy of any instructions, formulae, and drug doses should be independently verified with primary sources. The publisher shall not be liable for any loss, actions, claims, proceedings, demand, or costs or damages whatsoever or howsoever caused arising directly or indirectly in connection with or arising out of the use of this material.

Phase Equilibria in Mixtures Containing Polystyrene and Nematic Liquid Crystals

J. R. DORGAN and D. S. SOANE

Department of Chemical Engineering, University of California, Berkeley, Berkeley, CA 94720 U.S.A.

(Received January 18, 1990)

The phase behavior of two nematic liquid crystals in a polymer host is studied using the technique of Thermal Optical Analysis. Results are compared to the predictions of a recent molecular model due to Ballauff and found to give very good agreement for monodisperse polymers of sufficiently high molecular weight. Experimental findings include a widening of the two phase regime with increasing polymer chain length, exclusion of the polymer coils from the nematic phase and a sharp sensitivity of the phase behavior to the polydispersity of the polymer sample. All of these findings are in accord with the model and lend support to the general validity of the Flory-Ronca treatment of the anisotropic energetics responsible for thermotropic behavior.

Keywords: liquid crystal, phase behavior, statistical mechanics

INTRODUCTION

Many statistical theories of the nematic phase have been presented. Among the best known are those of Onsager,¹ Maier and Saupe,^{2,3} and Flory.⁴ The Onsager treatment has proven successful in the description of rigid molecules of high aspect ratio which display lyotropic behavior while the Maier-Saupe treatment has found application to lower aspect ratio molecules displaying thermotropic behavior.⁵ The extension of the original Flory lattice model to include anisotropic molecular forces by Flory and Ronca has created a theoretical framework which is particularly well suited for the description of mixtures containing nematogens.^{6,7,8}

This suitability arises from the factorization of the mixing partition function into combinatorial, orientational, and energetic terms. The combinatorial and orientation factors are arrived at through the usual probabilistic arguments involving the number of ways of arranging the substituents of the mixture on a lattice. Many such partition functions have been derived for a variety of mixtures including polydisperse rodlike particles and ternary systems consisting of solvent with either two rodlike components or one rodlike and one coillike component.^{9,10,11} These formulations have proven accurate in the description of athermal systems in which energetics play a secondary role to steric effects.¹²

Recently, the Flory-Ronca treatment has been extended by Ballauff to binary mixtures of random polymer coils and nematogens.¹³ These systems have potential for technological applications such as optical data storage media and display devices; the latter is particularly true for the droplet morphology shown in the photographs of Figure 1.¹⁴ In the original work, comparison between theory and experiment was made only for polymers of relatively low molecular weight. In this study, we present a comparison of the theory with experimental data for a much larger range of polymer molecular weight using two nematic molecules. One of these, 4'-Pentyl-4-biphenyl-carbonitrile (5CB), is of considerable interest in display device applications.

EXPERIMENTAL

Materials

Polystyrene was obtained from Polysciences Inc. and was near monodisperse, ($M_w/M_n < 1.05$). 4-(4-ethoxybenzylidene)-4-butylniline, (EBBA), obtained from Aldrich Chemical Co. was recrystallized until no change in melting temperature was detected, ($T_m = 40^\circ\text{C}$). 4'-Pentyl-4-biphenyl carbonitrile, (5CB), was obtained from Aldrich Chemical Co. and used as received.

Sample Preparation

Samples of varying composition were prepared by two separate methods. In each method, the material under study was weighed-out into clean sample vials. These vials were capped, sealed with paraffin film, and then heated to achieve miscibility. In the first method, this homogeneous mixture was removed immediately using a pipette and a small amount was placed on a microscope slide. A cover slide was then placed over the sample and sealed around its edges to the microscope slide using a quick-setting epoxy. The second method consisted of adding a minimum amount of 1,2-dichloroethane to the sample vial in order to form a room temperature stable homogeneous mixture. The solvent was selected for its volatility which allowed spin-coating of films onto cover slides. During this process the solvent flashed off leaving a thin-film two component mixture. The cover slide was again sealed to a microscope slide using a quick-setting epoxy. The advantage of the second method was its ability to produce uniform samples of well characterized thickness, (approximately 15 ± 5 microns). After it had been determined that both procedures gave identical experimental results, method two was used exclusively.

Apparatus

Cloud point curves for the two systems were determined using the technique of Thermal Optical Analysis, (TOA). The experimental apparatus is depicted in Figure 2. It consists of a polarizing microscope, (Nikon Optiphot-POL), equipped with a heating stage and photodiode, (Mettler FP80 system). An IBM PC-XT was used for data collection and storage. The experiment may be run in two comple-

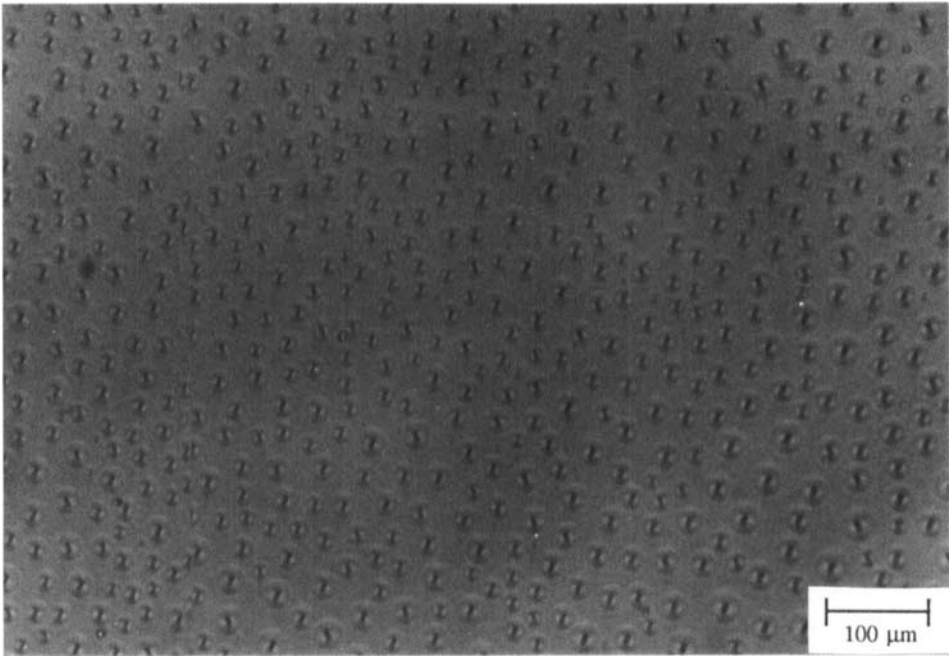


FIGURE 1A A mixture of EBBA and polystyrene in the two-phase region, viewed under linear polarization. The composition is 70% by weight of EBBA.

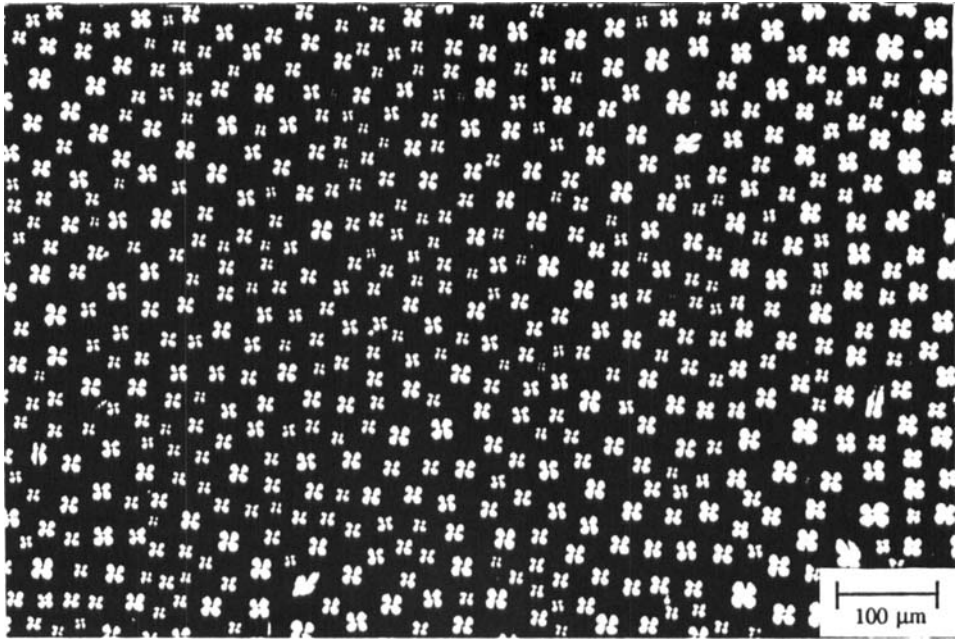


FIGURE 1B A mixture of EBBA and polystyrene in the two-phase region, viewed under crossed polarization. The composition is 70% by weight of EBBA.

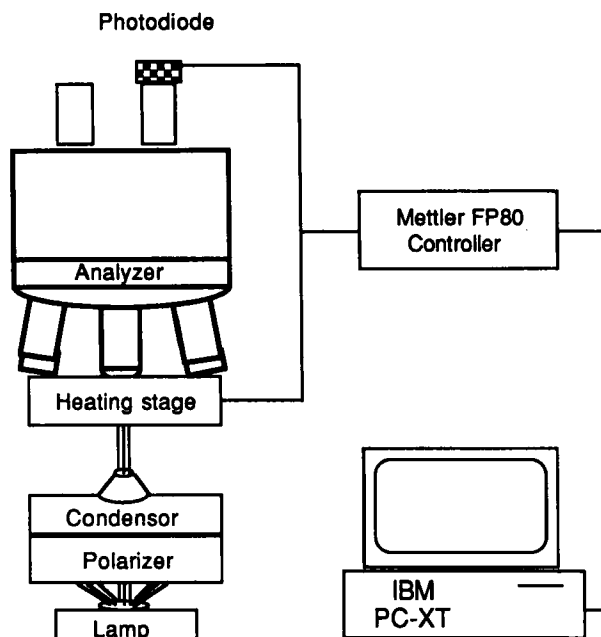


FIGURE 2 Schematic of experimental apparatus for cloud point determination using the technique of thermal depolarization analysis. The microscope used was a Nikon Optiphot-POL, transmitted light intensity vs. temperature data could be stored on the PC disk drives for subsequent analysis.

mentary configurations; with the polarizer and analyzer crossed or with them aligned. When the polarizers are crossed, the technique is also known as Thermal Depolarization Analysis, (TDA).¹⁵ As the temperature is either raised or lowered the light intensity transmitted through the sample is monitored by the photodiode. A two-phase sample, such as that shown in Figure 1A, scatters light much more strongly than a single phase. This causes a jump in the measured light intensity at the transition temperature when linear polarization is used. The cross-polarization configuration is particularly well suited for the systems studied. In an isotropic one-phase region, no light is transmitted and the photodiode reading is zero. If a nematic phase is present in the two-phase regime, light is transmitted through the crossed polarizers due to the birefringent nature of this phase.

The use of this optical method offered a significant advantage over the use of Differential Scanning Calorimetry, (DSC), which was initially investigated as a means for determining the phase behavior. Most importantly, it allowed the use of samples in the form of thin films. This expedited the kinetics of the phase separation process and eliminated major spatial or temporal inhomogeneities. Also, the amount of heat involved in the nematic-isotropic transition is small compared to melting; the same was found to be true for the demixing process studied here. Hence, the transition between one-phase and two-phases as measured by DSC was less sharp than in the method used in this study. Other problems with DSC for the study of liquid crystal phase transitions are discussed elsewhere [8].

Procedure

A sealed sample was placed in the microscope heating stage and heated to 100°C to achieve homogenization. The sample was then repeatedly heated and cooled over a temperature range near the clearing temperature of the pure nematogen while the light intensity was monitored. If the measured transition points upon heating and cooling agreed with each other, the point was taken as the equilibrium transition temperature. If these temperatures were different, slower heating and cooling rates were employed. For the two higher polymer molecular weights, by using a slow enough scan rate, agreement upon heating and cooling was always achieved. In the case of the lowest molecular weight, a slight discrepancy (less than 2°C) persisted despite the use of the slowest available scan rate, (0.2°C/min). This was true for both nematic molecules used in this study. In this case, the transition temperature upon cooling, corresponding to the traditional cloud point, has been taken as the equilibrium temperature. Figure 3 shows typical results for a 5CB-

5CB/PS ($M_w=22e3$) : 70/30

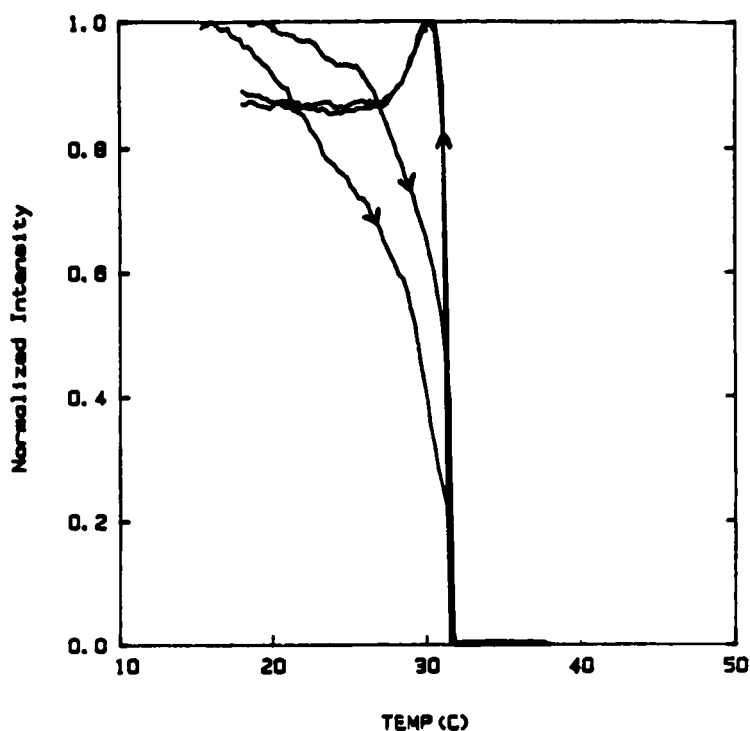


FIGURE 3 Typical experimental result. Normalized light intensity vs. temperature for a 70/30: 5CB/Polystyrene weight fraction sample. Arrows show the direction of temperature change. Two complete heating and cooling cycles are shown. The scan rate used was 0.2 K/min.

Polystyrene sample using the cross-polarization technique. For both systems studied, the intensity jump occurred at the same temperature independent of whether linear or crossed polarization was used.

Theoretical Background

We present here only a sketch of the theoretical formulation along with expressions for the chemical potentials of each component. The reader desiring a more detailed account is referred to the original references.^{6,10,13} The development of the theory proceeds along the lines of the aforementioned factorization of the partition function.

$$Z_M = Z_{\text{Comb}} Z_{\text{Orient}} Z_{\text{Config}} \quad (1)$$

It is subdivided into a combinatorial, an orientational, and configurational part. The last is taken as constant. Thus, this treatment excludes the possibility of any ordering effect of the nematic phase on the polymer coils residing therein.

The inclusion of anisotropic molecular dispersion forces is accomplished by introducing the mean energy of a rodlike segment, expressed as¹⁶:

$$\epsilon_\psi = - \left(\frac{k_B T^*}{\bar{V}} \right) \nu_r s \left(1 - \frac{3}{2} \sin^2 \psi \right) \quad (2)$$

For the entire system this energy is summed over all segment pairs.

$$E_{\text{Orient}} = - \frac{1}{2} n_r x_r \nu_r s^2 \left(\frac{k_B T^*}{\bar{V}} \right) \quad (3)$$

In the above, T^* is the characteristic temperature measuring the strength of the orientation dependent forces for a given nematic species.⁶ The order parameter, s , has its usual meaning; other quantities are defined in the Nomenclature column.

In this treatment, dipole effects are ignored. These forces scale with the order parameter rather than the order parameter squared. They may be included by the introduction of a second characteristic temperature. However, only one of these characteristic parameters may be calculated from the procedure described below.

Isotropic energetics may also be included in the form of a characteristic temperature for isotropic interaction.¹⁷

$$\Delta H_M = n_c x_c \nu_r \left(\frac{T_{\text{Iso}}^*}{T} \right) = n_c x_c \nu_r \chi \quad (4)$$

The connection between this second characteristic temperature and the familiar interaction parameter, χ , is given by the above equality. The interaction parameter, χ , is associated with the exchange energy of creating rodlike-coillike segment in-

teractions while destroying rodlike-rodlike and coillike-coillike segment interactions.¹⁸ Negative interaction parameters correspond to exothermic heats of mixing, that is, favorable mixing.

Formulation of the partition function in this manner gives the Helmholtz free energy and enables the derivation of the form of the distribution function, (see Appendix I). Subsequent differentiation with respect to species number gives the chemical potentials of the respective components.

The correct form of these equations is, (compare Reference 16):

$$\begin{aligned} \Delta\mu'_r/RT = & \ln \frac{v'_r}{x_r \bar{V}_r} + v'_r (\bar{y} - 1) + v'_c x_r \left(1 - \frac{\bar{V}_r}{\bar{V}_c x_c}\right) \\ & + x_r \left(\frac{\bar{V}_r}{\bar{V}'} - 1\right) + x_r (\bar{V}_r - 1) \left[a + \ln \left(1 - \frac{1}{\bar{V}'}\right) \right] - \ln f_1 \quad (5) \\ & - \frac{x_r v'_r s}{\bar{V}' \theta} \left[1 - \frac{1}{2} s - \frac{1}{2} s v'_r \left(1 - \frac{\bar{V}'}{\bar{V}_r}\right) + \frac{1}{2} s v'_c \right] + \chi v'^2_c \frac{\bar{V}_r x_r}{\bar{V}_c} \end{aligned}$$

$$\begin{aligned} \Delta\mu'_c/RT = & \ln \frac{v'_c}{x_c \bar{V}_c} + v'_r \frac{\bar{V}_c x_c}{\bar{V}_r x_r} (\bar{y} - 1) + v'_c \left(\frac{\bar{V}_c}{\bar{V}_r} x_c - 1\right) \\ & + x_c \bar{V}_c \left(\frac{1}{\bar{V}'} - \frac{1}{\bar{V}_r}\right) + \bar{V}_c x_c a + x_c (\bar{V}_c - 1) \ln \left(1 - \frac{1}{\bar{V}'}\right) \quad (6) \\ & + \frac{s^2 x_c}{2 \bar{V}' \theta} \frac{v'^2_r}{\bar{V}_r} (2 \bar{V}_c - \bar{V}') + \chi x_c v'^2_r \end{aligned}$$

and

$$\begin{aligned} \Delta\mu_r/RT = & \ln \frac{v_r}{x_r \bar{V}_r} + v_r (x_r - 1) + v_c x_r \left(1 - \frac{\bar{V}_r}{\bar{V}_c x_c}\right) \quad (7) \\ & + x_r \left(\frac{\bar{V}_r}{\bar{V}} - 1\right) + x_r (\bar{V}_r - 1) \ln \left(1 - \frac{1}{\bar{V}}\right) + \chi v^2_c \frac{\bar{V}_r x_r}{\bar{V}_c} \end{aligned}$$

$$\begin{aligned} \Delta\mu_c/RT = & \ln \frac{v_c}{x_c \bar{V}_c} + v_r \frac{\bar{V}_c x_c}{\bar{V}_r x_r} \left(1 - \frac{1}{x_r}\right) + v_c \left(\frac{\bar{V}_c}{\bar{V}_r} x_c - 1\right) \quad (8) \\ & + x_c \bar{V}_c \left(\frac{1}{\bar{V}} - \frac{1}{\bar{V}_r}\right) + x_c (\bar{V}_c - 1) \ln \left(1 - \frac{1}{\bar{V}}\right) + \chi x_c v^2_r \end{aligned}$$

In the above the prime represents quantities in an ordered phase, unprimed quantities represent those of an isotropic phase.

The order parameter, s , and disorientation index, \bar{y} , are defined in terms of the family of integrals, f_p .

$$\bar{y} = \frac{4}{\pi} x_r \left(\frac{f_2}{f_1} \right) \quad (9)$$

$$s = 1 - \frac{3}{2} \left(\frac{f_3}{f_1} \right) \quad (10)$$

where;

$$f_p = \int_0^{\frac{\pi}{2}} \sin^p \Psi \exp \left\{ -\frac{4}{\pi} x_r a \sin \Psi - \frac{3}{2} \left(\frac{x_r v_r s}{\bar{V} \theta} \right) \sin^2 \Psi \right\} d\Psi \quad (11)$$

The definition of the quantity, a , in the above is consistent with all previous work,

$$a = -\ln \left[1 - \frac{v_r}{\bar{V}_r} (1 - \bar{y}/x_r) \right] \quad (12)$$

Numerical Calculations

The characteristic temperature for anisotropic interactions, T^* , is accessible via the solution of the identity,

$$\Delta\mu'_r = \Delta\mu_r \quad (13)$$

for a pure component at the nematic-isotropic transition temperature. Details of the calculation are given in Reference [13]. The needed molecular parameter along with the calculated values of T^* appear in Table I. For 5CB, the nematic-isotropic transition temperature was measured in our laboratory using TOA. The aspect ratio was calculated from x-ray diffraction studies of a related compound.¹⁹ The value arrived at compares favorably with the value, $x_r = 3.1$, found from the molar hard core volume and minor axis diameter of the compound. The thermal expansion coefficient was determined from the volumetric data of Reference [20]. For EBBA, the nematic-isotropic transition temperature was also measured in our laboratory. The needed equation of state data for this molecule was adopted from previous work.¹³

Temperature-Composition phase diagrams may be found through the solution for the rodlike component volume fractions from the equilibrium conditions, $\Delta\mu'_i = \Delta\mu_i$, for each species.¹³ Figure 4 shows the effect of molecular weight for a hypothetical system where the rodlike component aspect ratio is taken as 4.0 and the nematic-isotropic transition temperature is arbitrarily set to 100°C. For $x_c \geq 50$, the nematogen rich phase approaches complete exclusion of the random coil.

TABLE I

Equation of state data for materials studied

EBBA (4-(4 Ethoxybenzylidene)-4-butylaniline):

$x_r = 3.7$	$T_{ni} = 80\text{ }^{\circ}\text{C}$	$\rho(80^{\circ}\text{C}) = 0.9881\text{ g/cm}^3$
$\alpha = 8.22 \times 10^{-4}\text{ 1/K}$	$T^* = 351.2\text{ K}$	$V^* = 229.3\text{ cm}^3/\text{mol.}$

5CB(4-Pentyl-4-biphenyl-carbonitrile):

$x_r = 3.3$	$T_{ni} = 34.9\text{ }^{\circ}\text{C}$	$\rho(35^{\circ}\text{C}) = 0.9900\text{ g/cm}^3$
$\alpha = 1.00 \times 10^{-3}\text{ 1/K}$	$T^* = 371.4\text{ K}$	$V^* = 200.7\text{ cm}^3/\text{mol.}$

This leads to a numerical difficulty for higher molecular weights as the nematic rich phase composition exceeds the number of repeating units available as significant digits in double precision FORTRAN. For the calculations involving this hypothetical system, this difficulty was overcome through the use of quadruple precision FORTRAN.

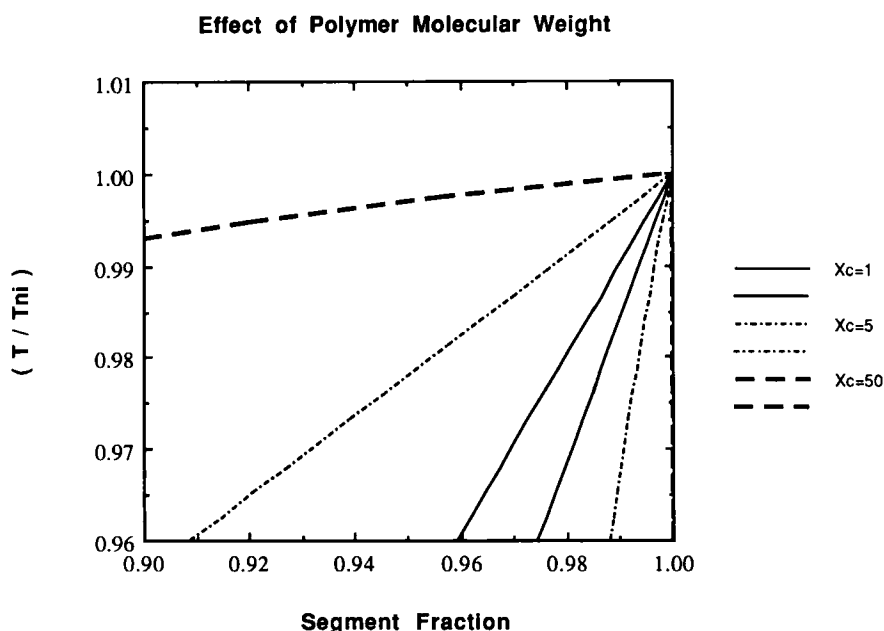


FIGURE 4 Widening of the biphasic region with increasing coil molecular weight. For high enough values, the polymer is completely excluded from the nematic phase. The independent variable is the segment fraction of the nematic species, the temperature is reduced by the clearing temperature of the pure compound. The model reduces to a nematic in solution when the contour length of the coil is taken as unity.

Figure 5 shows the effects of the isotropic energetics term on the phase behavior. As expected, a negative interaction parameter narrows the biphasic regime while a positive value widens this region. The magnitude of T_{iso}^* used in these calculations corresponds to an interaction parameter with an absolute value of approximately 0.11. Under these conditions there is no possibility of isotropic-isotropic demixing prior to isotropic-nematic demixing.

Comparison with Real Systems

We turn now to the comparison of model predictions with the actual observed phase behavior. For the highest molecular weight system studied, $M_w = 113,000$, exact solution of the conditions for equilibrium was not possible. This was due to the demand for significant figures discussed above. The calculations were accordingly performed by setting the composition of the ordered phase to unity and solving one remaining equation for the isotropic phase composition. The application of this method to the next lower molecular weight system, $M_w = 22,000$, gave results that agreed with the exact solution using quadruple precision FORTRAN to six significant figures. Figure 6 shows the comparison of model predictions to measured cloud point curves for the lowest molecular weight polystyrene, ($M_w = 4,000$). This system displayed no experimental evidence of a nematic phase with a finite polymer concentration, only one transition was measured over the range of temperatures shown. These findings are in agreement with the model which predicts complete exclusion of the polymer coil for this molecular weight. Figures 7 and 8 show the results for even higher molecular weights, ($M_w = 22,000$ and $M_w = 113,000$). We see immediately that the agreement is excellent for these higher

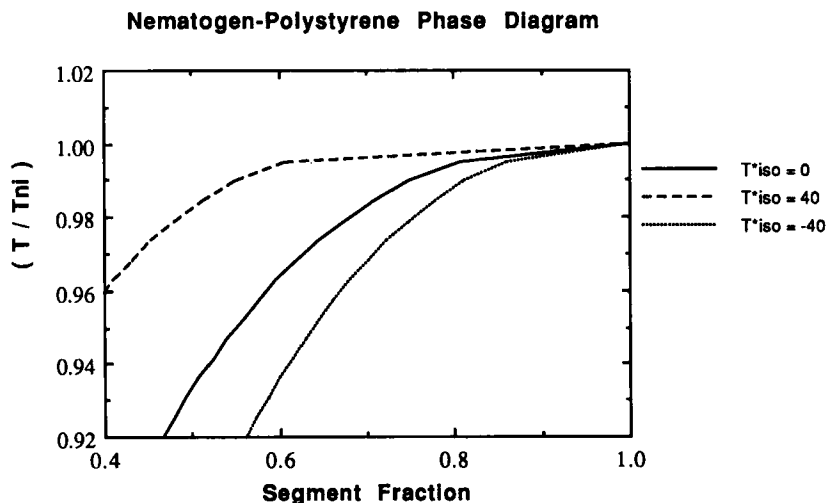


FIGURE 5 Phase diagram for nematogen and polymer coil demonstrating the effects of the interaction parameter. The axial ratio of the nematic species is taken as 4.0, its thermal expansion coefficient as $8.0 \times 10^{-4} \text{ 1/K}$, and its nematic-isotropic transition temperature as 100°C . This results in a characteristic temperature of $T^* = 330.5 \text{ K}$. The properties of the polymer coil reflect those of polystyrene with $M_w = 22,000$. The ordinate has been reduced by the nematic-isotropic transition temperature of the pure component. The abscissa is the segment fraction of the nematic species.

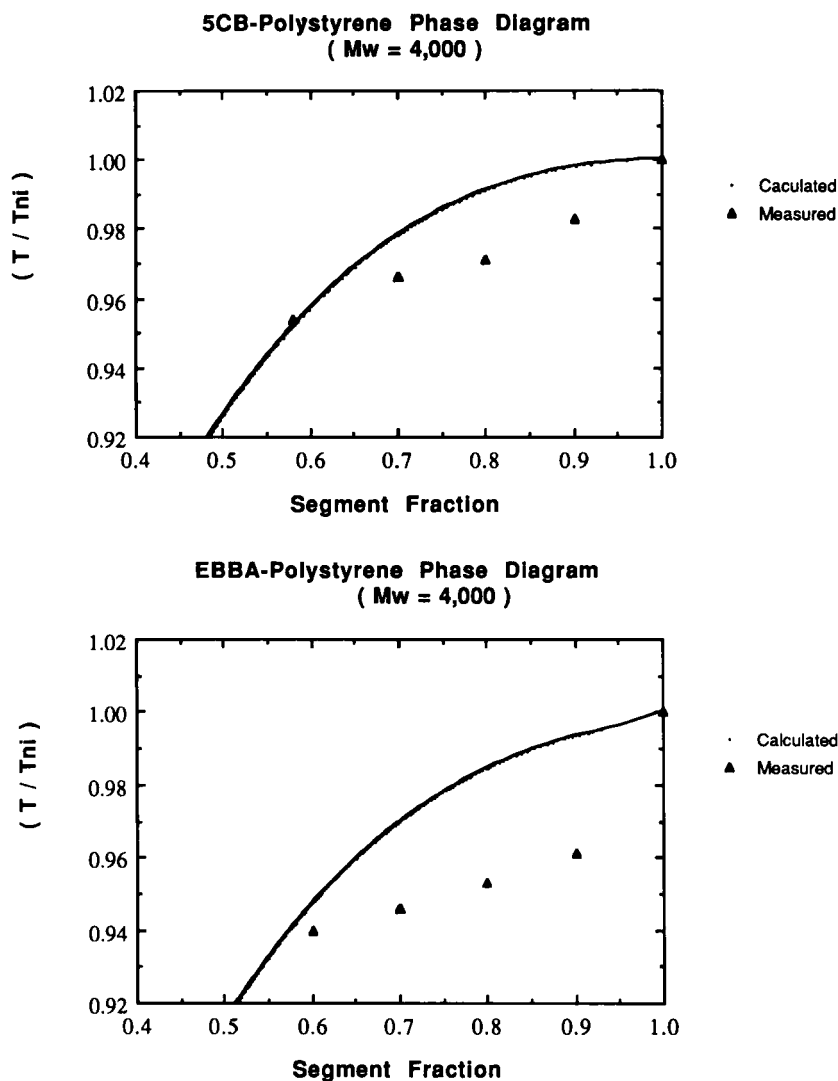


FIGURE 6 Comparison of theory with experiment for two nematic molecules using no adjustable parameters. The temperature axis has been reduced by the pure component clearing temperature. The segment fraction of the nematic species is taken as the independent variable.

molecular weight systems. This is particularly true for the 5CB system. It should be emphasized that the predictions shown in Figures 6–8 have been accomplished *without any adjustable parameters*.

DISCUSSION

The lattice model gives excellent results for high polymer molecular weights as expected. This is because as x_c increases, the phase behavior becomes dominated by entropy effects. The agreement achieved is therefore validation of the lattice

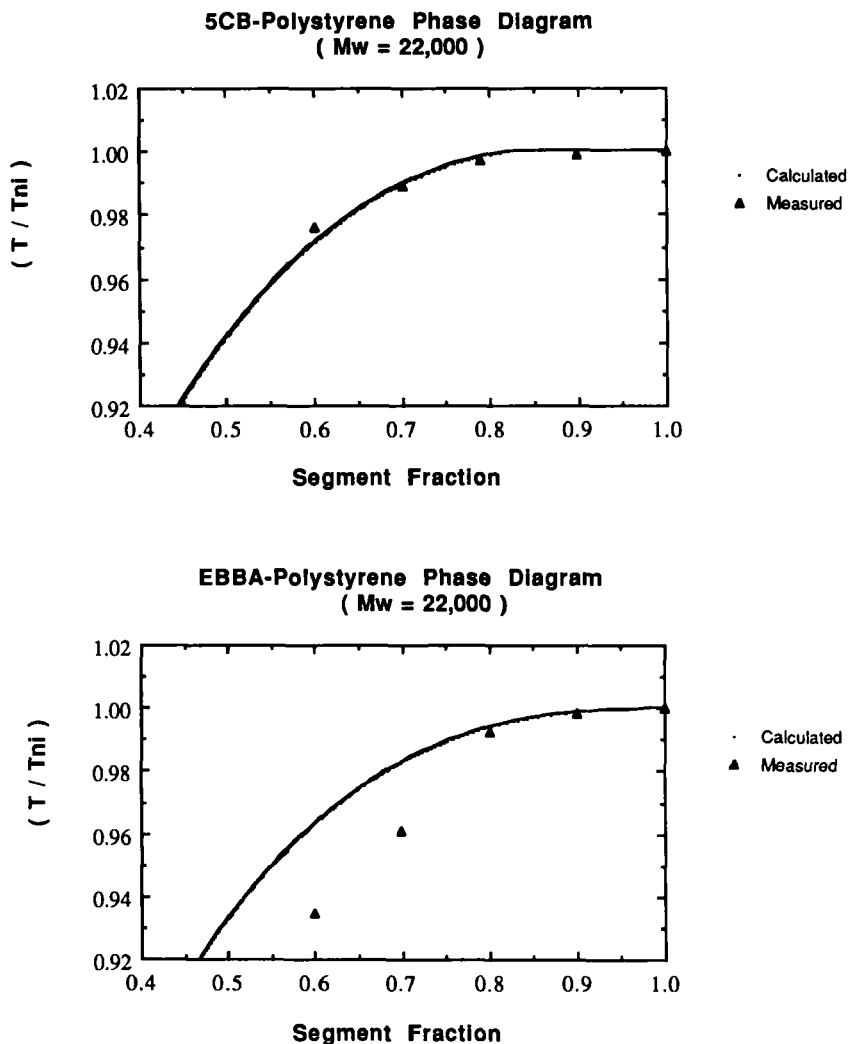


FIGURE 7 Comparison of theory with experiment for two nematic molecules using no adjustable parameters. The temperature axis has been reduced by the pure component clearing temperature. The segment fraction of the nematic species is taken as the independent variable.

treatment in describing the entropic contributions to the free energy for polymers of sufficiently high molecular weight.

For 5CB, the characteristic temperature of anisotropic interaction, T^* , is much higher than that for EBBA. The ability of the model to accurately describe the phase behavior of the 5CB-polystyrene system using a zero valued interaction parameter should not be confused with truly athermal behavior. The latter implies that there are no energetic terms of significance and that the phase behavior is completely determined by entropy considerations. Such a view is inconsistent with the observed thermotropic behavior. It is a tradeoff between unfavorable entropy

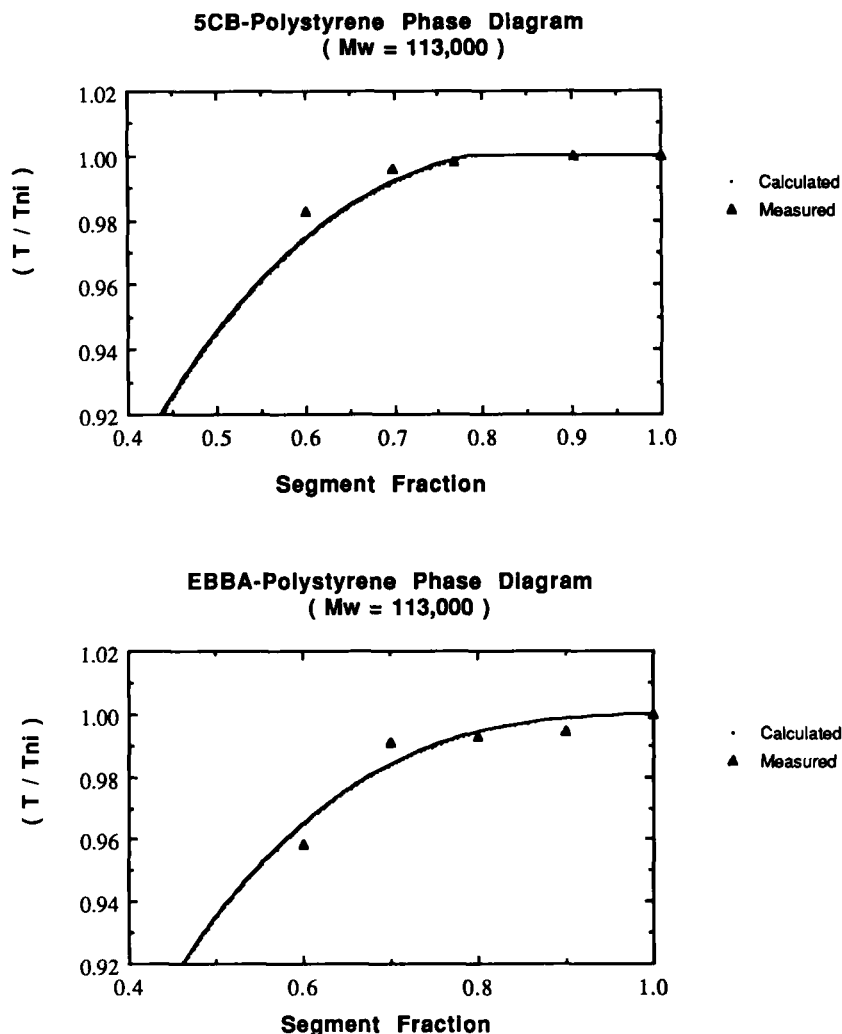


FIGURE 8 Comparison of theory with experiment for two nematic molecules using no adjustable parameters. The temperature axis has been reduced by the pure component clearing temperature. The segment fraction of the nematic species is taken as the independent variable.

contributions and favorable energetic contributions to the free energy which leads to the formation of an ordered phase at some critical temperature. The net result of forming very favorable rod-rod segment interactions at the expense of rod-coil segment interactions is a zero χ . The system is exhibiting *compensating effects*. Clearly, this must be regarded as fortuitous. The interaction parameter includes an energetic contribution from forming favorable contacts between rodlike segments. In the absence of rod-coil segment interactions, we would expect a positive interaction parameter or equivalently an endothermic heat of mixing. This is due to the fact that miscibility may be accomplished only through the destruction of the favorable energetics which stabilize the nematic phase.

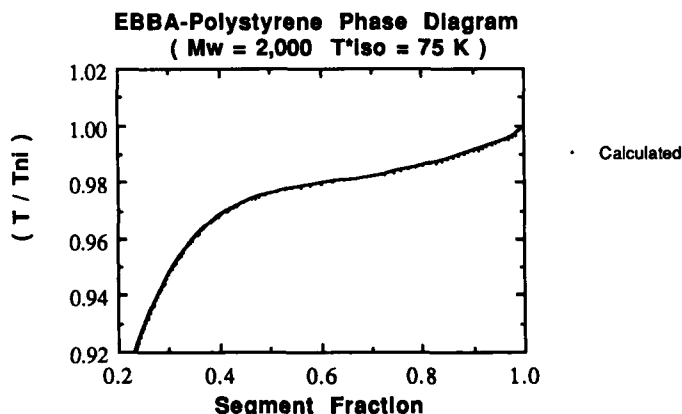


FIGURE 9 Hypothetical phase diagram which displays the experimentally observed concavity in low molecular weight polymer systems. The molecular weight of the coil is taken as 2,000. A value of 75 K is assumed for the characteristic temperature of isotropic interaction.

Examination of the comparison between theory and experiment for the lowest molecular weight polystyrene is less satisfactory. The theory fails to predict the correct shape of the two phase region. It should be noted that the cloud point results for the lowest molecular weight system are less accurate than for the other systems. The failure to achieve the same transition temperature upon heating and cooling most likely indicates fractionation of chains of varying molecular weight. This interpretation is supported by the findings of a preliminary study we conducted where a polydisperse sample of polystyrene of roughly $M_w = 20,000$ was used.²¹ It was not possible to achieve agreement between heating and cooling transition temperatures with this sample. While the low molecular weight polystyrene was stored under refrigeration in our laboratory, it was shipped at ambient conditions and may have undergone changes in its molecular weight distribution during this period. It is to be noted, however, that previous workers have reported on the EBBA and low molecular weight polystyrene system and they also found this type of concavity in the phase diagram.²²

Figure 9 shows a hypothetical calculation for EBBA and polystyrene. Here the molecular weight of the polystyrene is taken as $M_w = 2,000$ and a value of 75 K for the characteristic temperature of isotropic interaction is assumed. We see that the theory is capable of producing the observed shape of the experimentally determined phase diagram with these parameter values. While such a low value of the molecular weight of the polymer sample cannot be justified, the theory is capable of describing all of the observed phase behavior in a semi-quantitative manner.

CONCLUSIONS

The molecular model of Ballauff for a system of thermotropic rods and random polymer coils is rigorously tested against experimental data. It is found that the model predicts many of the salient features of these systems. These include a

widening of the two phase regime with increasing molecular weight, exclusion of the polymer coils from the nematic phase and a sharp sensitivity of the phase behavior to the polydispersity of the polymer sample.

It is established that Thermal Depolarization Analysis provides an excellent method for studying phase behavior in mixtures containing nematic molecules. This method offers some significant advantages over the use of Differential Scanning Calorimetry.

The theory overpredicts the effects of molecular weight for mixtures containing polymers of low molecular weight. Very good agreement between theory and experiment is found for mixtures containing polymers of sufficiently high molecular weight. In one system studied, (5CB-polystyrene), excellent predictions were made without the use of any adjustable parameters. This is a fortuitous result. *The general description of these mixtures requires the use of one additional adjustable energetics parameter.* The experimental findings on the second system studied (EBBA-polystyrene) support this conclusion.

The theory of Ballauff^{13, 16, 17} based on the previous work of Flory¹¹ and Flory and Ronca⁶ is capable of describing all of the observed phase behavior in two systems experimentally studied. The quantitative agreement possible for polymers of sufficiently high molecular weight lends strong support both to the applicability of the lattice formulation of the entropy of mixing and to the validity of the Flory-Ronca treatment of the anisotropic energetics responsible for thermotropic behavior.

Acknowledgments

This work was supported by the National Science Foundation via grant CBT-8714420. J.R.D. gratefully acknowledges the Fannie and John Hertz Foundation for a Hertz Fellowship.

Nomenclature:

A	—	Helmholtz free energy
E_{Orient}	—	orientational energy of the system as a whole.
$f(\Psi)$	—	distribution function.
H_M	—	enthalpy of mixing.
k_B	—	Boltzmann's constant.
n_0	—	number of vacancies on the lattice.
n_c	—	number of coillike molecules.
n_r	—	number of rodlike molecules.
R	—	gas constant.
s	—	order parameter.
T	—	absolute temperature.
T_{ni}	—	nematic-isotropic transition temperature.
T^*	—	characteristic temperature of anisotropic interaction.
T_{Iso}^*	—	characteristic temperature of isotropic interaction.
V^*	—	molar hardcore volume.
\bar{V}	—	reduced volume of the mixture.

\bar{V}_c	—	reduced volume of the coillike component.
\bar{V}_r	—	reduced volume of the rodlike component.
ν_c	—	volume fraction of coillike component.
ν_r	—	volume fraction of rodlike component.
x_c	—	contour length of the polymer chain.
x_r	—	aspect ratio of rodlike component.
\bar{y}	—	Flory disorientation parameter.
Z_{Comb}	—	combinatoric partition function.
Z_{Config}	—	configurational partition function.
Z_M	—	mixing partition function.
Z_{Orient}	—	orientational partition function.
α	—	thermal expansion coefficient.
δ	—	variational operator.
ϵ_Ψ	—	average energy of a segment at orientation Ψ .
Ψ	—	angle between rod axis and preferred axis.
ρ	—	density.
χ	—	interaction parameter.
μ_c	—	chemical potential of the coillike component.
μ_r	—	chemical potential of the rodlike component.
θ	—	reduced temperature, (T/T^*) .

Appendix I: Derivation of the Distribution Function

The free energy function proposed by Ballauff for a mixture of thermotropic rods and flexible polymer coils may be recast in the form of a functional. This allows use of the variational calculus to determine the form of the distribution function of the rods at equilibrium. The Helmholtz free energy is expressed as a double integral over the angular phase space and the total number of lattice elements.

$$\begin{aligned}
 \frac{A}{kT} = & \int_0^{n_0} \frac{dn}{n} \int_0^{\pi/2} -\frac{4}{\pi} x_r n_r f(\Psi) \ln \left[1 - \frac{n_r x_r}{n_o} (1 - \bar{y}/x_r) \right] \cdot \\
 & \sin \Psi + \frac{3}{2} \frac{(n_r x_r)^2}{n_o \theta} \frac{\bar{V}_r}{\bar{V}} s \sin^2 \Psi f(\Psi) \\
 & + \left[n_r \ln \left(\frac{n_r}{n_o} \right) + n_c \ln \left(\frac{n_c}{n_o} \right) + n_c (x_c - 1) + (n_o - n_r x_r - n_c x_c) \cdot \right. \\
 & \left. \ln [(n_o - n_r x_r - n_c x_c)/n_o] \right] \cos \Psi \\
 & + n_c x_c \chi \bar{V}_n \left(\frac{n_r x_r}{n_r} \right) \cos \Psi + n_r f(\Psi) \ln [f(\Psi)/\omega_y] d\Psi
 \end{aligned} \quad (1)$$

The criterion for a minimum energy state is that the first variation of the functional is zero taking into account the restraint that the species present must be conserved.

Introducing the Lagrange multipliers, μ_i , we have:

$$\delta_1 = \delta \left(\frac{A}{kT} - \mu_r \int_0^{n_0} \frac{dn}{n} n_r - \mu_c \int_0^{n_0} \frac{dn}{n} n_c \right) = 0$$

The variation is calculated in a fashion analogous to finding a differential using the chain rule. The above integral is differentiated with respect to the independent variables, each partial derivative being multiplied by the variation of that variable. For simplicity, let us denote the above integrand as I ; the free energy is conveniently expressed as,

$$\frac{A}{kT} = \int_0^{n_0} \frac{dn}{n} \int_0^{\pi/2} I(f, n_r, n_c) d\Psi$$

The first variation may now be calculated.

$$\begin{aligned} \delta_1 = \int_0^{n_0} \frac{dn}{n} \int_0^{\pi/2} \left(\frac{\partial I}{\partial f} \right) \delta f + \left[\left(\frac{\partial I}{\partial n_r} \right) - \mu_r \cos \Psi \right] \delta n_r \\ + \left[\left(\frac{\partial I}{\partial n_c} \right) - \mu_c \cos \Psi \right] \delta n_c d\Psi \end{aligned}$$

Rearrangement gives,

$$\begin{aligned} \delta_1 = \int_0^{n_0} \left[\int_0^{\pi/2} \left(\frac{\partial I}{\partial n_r} \right) d\Psi - \mu_r \right] \delta n_r \frac{dn}{n} + \int_0^{n_0} \left[\int_0^{\pi/2} \left(\frac{\partial I}{\partial n_r} \right) d\Psi - \mu_r \right] \\ \delta n_r \frac{dn}{n} + \int_0^{n_0} \int_0^{\pi/2} \left(\frac{\partial I}{\partial f} \right) \delta f d\Psi \frac{dn}{n} \end{aligned}$$

The variations which appear within the integrals are arbitrary. All three double integrals must vanish independently. The criterion of a vanishing first variation is therefore given by the three relations,

$$\mu_c = \int_0^{\pi/2} \left(\frac{\partial I}{\partial n_c} \right) d\Psi \quad \mu_r = \int_0^{\pi/2} \left(\frac{\partial I}{\partial n_r} \right) d\Psi \quad \left(\frac{\partial I}{\partial f} \right) = 0$$

As usual, the Lagrangian multipliers are associated with the chemical potentials. Application of the third relationship to the functional form given above yields,

$$\begin{aligned} -\frac{4}{\pi} x_r n_r \ln \left[1 - \frac{n_r x_r}{n_o} (1 - \bar{y}/x_r) \right] \sin \Psi + \frac{3}{2} \frac{(n_r x_r)^2}{n_o \theta} \frac{\bar{V}_r}{\bar{V}} s \sin^2 \Psi \\ + \left[1 + \ln \left(\frac{f(\Psi)}{\omega_y} \right) \right] = 0 \end{aligned}$$

Upon rearrangement, this gives:

$$f(\Psi) = \omega_y \exp \left\{ -\frac{4}{\pi} x_r n_r \ln \left[1 - \frac{n_r x_r}{n_o} (1 - \bar{y}/x_r) \right] \cdot \sin \Psi \right. \\ \left. + \frac{3}{2} \frac{(n_r x_r)^2}{n_o \theta} \frac{\bar{V}_r}{\bar{V}} s \sin^2 \Psi - 1 \right\}$$

The arbitrary constant is removed upon normalization, the association of ω_y with $\sin \Psi$ was demonstrated by Flory and Ronca.⁶ The final form of the distribution function follows as:

$$f(\Psi) = \sin \Psi \exp \left\{ -\frac{4}{\pi} x_r n_r \ln \left[1 - \frac{n_r x_r}{n_o} (1 - \bar{y}/x_r) \right] \cdot \sin \Psi \right. \\ \left. + \frac{3}{2} \frac{(n_r x_r)^2}{n_o \theta} \frac{\bar{V}_r}{\bar{V}} s \sin^2 \Psi \right\}$$

References

1. L. Onsager, *Ann. N.Y. Acad. Sci.*, **51**, 627 (1949).
2. W. Maier and A. Saupe, *Z. Naturforschg*, **14a**, 882 (1959).
3. W. Maier and A. Saupe, *Z. Naturforschg*, **15a**, 287 (1960).
4. P. J. Flory, *Proc. Royal Soc., London, Ser. A*, **234**, 73 (1956).
5. Chandrasekhar, *Liquid Crystals*, Cambridge University Press, Cambridge (1977).
6. P. J. Flory and G. Ronca, *Mol. Cryst. Liq. Cryst.*, **54**, 311 (1979).
7. P. J. Flory and P. Irvine, *J. Chem. Soc. Faraday Trans. I*, **80**, 1807 (1984).
8. M. Ballauff and P. J. Flory, *Ber. Bunsenges Phys. Chem.*, **88**, 530 (1984).
9. P. J. Flory and A. Abe, *Macromolecules*, **11**, 1119 (1978).
10. P. J. Flory and A. Abe, *Macromolecules*, **11**, 1121 (1978).
11. P. J. Flory, *Macromolecules*, **11**, 1138 (1978).
12. W. F. Hwang, D. R. Wiff, C. L. Benner and T. E. Helminiak, *J. Macromol. Sci. Phys. B*, **22**(2), 231 (1983).
13. M. Ballauff, *Mol. Cryst. Liq. Cryst.*, **136**, 175 (1986).
14. J. M. Doane, N. A. Vaz, B. G. Wu and S. Zumer, *Appl. Phys. Lett.*, **48**, 269 (1986).
15. N. Hartshorne, *The Microscopy of Liquid Crystals*, Microscope Publications Ltd. London 1974.
16. M. Ballauff, *Ber. Bunsenges Phys. Chem.*, **90**, 1053 (1986).
17. M. Ballauff, *Mol. Cryst. Liq. Cryst. Letters*, **4**(1), 15 (1986).
18. P. J. Flory, *Principles of Polymer Chemistry*, Cornell University Press, Ithaca, N.Y. (1953).
19. P. Mandel, S. Paul, H. Schenk and K. Gaubitz, *Mol. Cryst. Liq. Cryst.*, **135**, 35 (1986).
20. T. Shirakawa, T. Hayakawa, and T. Tokuda, *J. Phys. Chem.*, **87**, 1406 (1983).
21. J. R. Dorgan and D. S. Soane, Unpublished.
22. B. Kronberg, I. Bassignana and D. Patterson. *J. Phys. Chem.*, **82**, 1714 (1978).